

Photosensitized Oxidation of ^{13}C , ^{15}N -Labeled Imidazole Derivatives

Ping Kang and Christopher S. Foote*

Contribution from the Department of Chemistry and Biochemistry, University of California, Los Angeles, Los Angeles, California 90095-1569

Received September 27, 2001. Revised Manuscript Received February 26, 2002

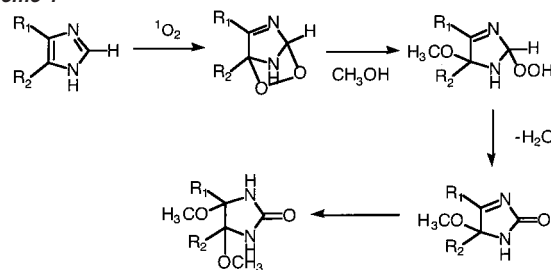
Abstract: An efficient synthesis of imidazoles with isotope labeling at different positions of the five-membered ring was developed. We carried out a detailed mechanistic study of the photosensitized oxidation of isotope-labeled imidazole derivatives. A new product, CO_2 , was observed in the photooxidation of 2-H,N1-H imidazoles, but not in 2-substituted imidazoles. The carbon of CO_2 derives from the 2C of imidazole. As shown by ^{18}O experiments, both oxygen atoms of CO_2 originate mainly from one molecule of oxygen. Transient intermediates were detected by low-temperature NMR in the photosensitized oxidation of the isotope-labeled imidazoles. Quantitative analysis of the ^{13}C NMR at different temperatures and times correlates the formation of one intermediate with the loss of another, thus allowing the complete decomposition pathway of the transient intermediates to be established. Singlet oxygen reacts with 4,5-diphenylimidazole via a [4 + 2] cycloaddition to form a 2,5-endoperoxide, which, upon warming, decomposes to a hydroperoxide. The hydroperoxide in one pathway loses water to form an imidazolone **7**, which is hydrolyzed to a hydroxyimidazol-2-one **11**. In another pathway, the hydroperoxide rearranges to diol **8**. The diol rearranges to a carbamate **9** by opening and reclosing the five-membered ring. **9** decomposes to CO_2 and benzil diimine. A labile NH in the imidazole is crucial for the decomposition of the initially formed endoperoxide, otherwise the endoperoxide decomposes to regenerate starting material. Many similarities exist between the photooxidations of imidazole and guanosine in organic solvent, suggesting that the two reactions share a similar reaction mechanism with singlet oxygen.

Introduction

Imidazole structures exist in many purines such as guanosine, xanthine, theophylline, and 8-methylcaffeine, and the reactions with singlet oxygen take place by attack on the imidazole portion.¹ Studies of imidazole model systems should also help to clarify the mechanism of imidazole breakdown in enzyme deactivation by photosensitized oxidation. It has been shown that histidine (His) destruction by singlet oxygen can be correlated with loss of biological activity of His containing enzymes.² Mechanistic studies strongly indicate that the photooxidation of His involves singlet oxygen and that the target of the oxidation is the imidazole ring of the His residue.

Wasserman and co-workers carried out extensive studies on a variety of alkyl and aryl-substituted imidazoles.^{3,4} The

Scheme 1



proposed major reaction pathway with singlet oxygen is shown in Scheme 1. In these studies, CH_3OH was the reaction medium as well as the trapping agent for intermediates. The endoperoxide was proposed to be the initially formed product. The final product was the methanol adduct.

Products from the photosensitized oxidation of various imidazole derivatives and their yields were reported previously^{3,5–7} and have been compiled by Wasserman et al.⁴ The total yields of the isolated products from photooxidation of 2-H-imidazole derivatives are quite low (9–35%), which implies that many products are not identified in such reactions. Irie and co-workers reported 17 compounds from the photosensitized oxidation of

* To whom correspondence should be addressed. E-mail: foote@chem.ucla.edu.

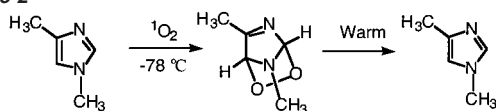
- (1) Matsuura, T.; Saito, I. *J. Chem. Soc. Chem. Commun.* **1967**, 693; Matsuura, T.; Saito, I. *Tetrahedron Lett.* **1968**, 29, 3273; Matsuura, T.; Saito, I. *Tetrahedron* **1968**, 24, 6609; Matsuura, T.; Saito, I. *Tetrahedron* **1969**, 25, 541–547; Matsuura, T.; Saito, I. *Tetrahedron* **1969**, 25, 549–556; Matsuura, T.; Saito, I. *Tetrahedron* **1969**, 25, 557–564.
- (2) Chang, S. H.; Teshima, G. M.; Milby, T.; Gillette-Castro, B.; Canova-Davis, E. *Anal. Biochem.* **1997**, 244, 221–227; Morikawa, S. Y.; Kanatani, A.; Yoshimoto, T.; Tsuru, D. *Agric. Biol. Ch.* **1991**, 55, 2099–2103; Kuno, S.; Fukui, S.; Toraya, T. *Arch. Biochem. Biophys.* **1990**, 277, 211–217; Henschen-Edman, A. H. *Cell. Mol. Life Sci.* **1997**, 53, 29–33; Micanovic, R.; Procyk, R.; Lin, W. H.; Matsueda, G. R. *J. Biol. Chem.* **1994**, 269, 9190–9194.
- (3) Wasserman, H. H.; Druckrey, E. *J. Am. Chem. Soc.* **1968**, 90, 2440.
- (4) Wasserman, H. H.; Lipschutz, B. H. In *Singlet Oxygen*; Wasserman, H. H., Murray, R. W., Eds.; Academic Press: New York, 1979; pp 430–510.

(5) Wasserman, H. H.; Stiller, K.; Floyd, M. B. *Tetrahedron Lett.* **1968**, 29, 3277–3280.

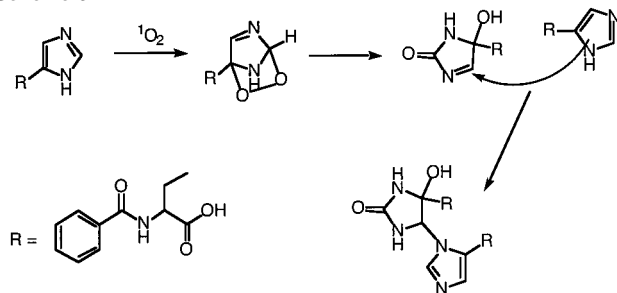
(6) White, E. H.; Harding, M. J. C. *J. Am. Chem. Soc.* **1964**, 86, 5686.

(7) Sonnenberg, J.; White, D. M. *J. Am. Chem. Soc.* **1964**, 86, 5685.

Scheme 2



Scheme 3



N-benzoyl histidine at pH 11.⁸ In contrast, the total yields of the products from 2-H-substituted imidazole derivatives are much higher (42%–97%).

Foote and co-workers reported low-temperature NMR studies of photosensitized oxidation of imidazoles and observation of 2,5-endoperoxides as initial oxidation products.⁹ The intermediates have been shown to undergo several subsequent reactions, depending on the substrates. In some cases, the initial adduct lost oxygen to regenerate starting material. (Scheme 2)

The photosensitized crosslinking of proteins is involved in the photodynamic therapy (PDT) of tumors and other diseases.¹⁰ His-His crosslinking plays a role in the photosensitized crosslinking of proteins mediated by singlet oxygen.¹¹ His can also crosslink with Lys, Cys, Trp, Tyr, and even Arg on photosensitized treatment. Kopecek et al. reported the formation of His-His crosslinks in the photosensitized oxidation of N-benzoyl-L-histidine (Bz-His).¹² A mechanism for the formation of the crosslink was proposed in which the first step was the 1,4-cycloaddition of singlet oxygen to the Bz-His imidazole ring to give an unstable endoperoxide. The endoperoxide rearranged by nucleophilic addition and the elimination of one water molecule to give the crosslinked product. (Scheme 3)

In a previous mechanistic study of the photosensitized oxidation of guanosine,¹³ we detected two transient intermediates from an 8-¹³C-labeled guanosine derivative by low-temperature NMR. However, no precursors to the two observed transient intermediates could be detected directly even down to -100 °C, which suggests that any such precursors are very unstable. We also identified CO₂ as a major product that comes from the 8-position (C2 of the imidazole ring; CO₂ was also formed from other carbons, probably C6) of guanosine. Because of the structural similarity of imidazole and guanosine, we looked for reports of CO₂ formation in the photosensitized oxidation of imidazole but found none,^{5,9,14} which suggests the reaction

leading to CO₂ is a novel reaction pathway and that more detailed studies of the photooxidation of imidazoles are needed.

In this contribution, we report the synthesis of ¹³C,¹⁵N-labeled 4,5-diphenylimidazole derivatives and their low-temperature photosensitized oxidation. A series of transient intermediates was detected using low-temperature NMR. A detailed reaction mechanism was deduced from this study. A preliminary account of the synthesis of a few of these compounds and a partial study of their reactions has appeared.¹⁵

Results

CO₂ Formation. Since no CO₂ formation was reported in previous studies of photosensitized oxidation of imidazole derivatives but we found CO₂ to be a major product of the oxidation of guanosine, our first attempt was to look for CO₂ formation. The photosensitized oxidation of imidazole derivatives was carried out in a 5-mm NMR tube at -80 °C in acetone-*d*₆ with ca. 5×10^{-5} M of 2,9,16,23-tetra-*tert*-butyl-19*H*,31*H*-phthalocyanine as sensitizer and a Cermax 300-W xenon lamp as the light source. A chromium glass filter was used to cut off wavelengths below 547 nm. After 1 h of photolysis, the reaction mixture was allowed to warm to room temperature. CO₂ formation, was shown by GC/MS.

Several imidazole derivatives were tested for CO₂ formation and the results are shown in Table 1. These compounds can be categorized into two groups. The first group consists of 4,5-diphenylimidazole (entry 1), 4-methylimidazole (entry 2), and imidazole (entry 3), which are 2-H,N1-H-derivatives. Comprising the second group are 2-substituted (entry 6) or N1-substituted (entries 4, 5) or 2,N1-disubstituted (entry 7). CO₂ was detected from all the imidazoles in the first group, while very little or none was detected from the second group. These results strongly suggest that the rearrangement of N1-H and 2-H of the imidazole ring are necessary for the formation of CO₂ in the photosensitized oxidation of imidazole derivatives.

The carbon atom in CO₂ originates from the C2 of the imidazole ring. ¹³CO₂ (*m/z* 45) was shown by GC/MS from the photosensitized oxidation of 2-¹³C-4,5-diphenylimidazole. Formation of ¹³CO₂ was also confirmed by observation of a ¹³C NMR peak at 124.0 ppm.

The origin of the two oxygen atoms of CO₂ was studied in an ¹⁸O experiment. The three substrates used in this experiment were 4,5-diphenylimidazole, 4-methylimidazole, and imidazole. The resulting CO₂ was analyzed by MS, and the distributions of CO₂ isotopes are shown in Table 2. A substantial amount of ⁴⁸[CO₂] was observed in the photosensitized oxidation of all three substrates. The experimental distributions do not exactly match the calculated values for either the case where both O atoms of CO₂ derive from the same O₂ molecule (2-O in Table 2) or the case where they come from two different O₂ molecules (1-O in Table 2). However, they are closer to the values for 2-O than 1-O. The calculated ⁴⁸[CO₂] values are 1.9–2.6 times larger than experimental ⁴⁸[CO₂] for 2-O for all three substrates, but 7–13 times smaller for 1-O. If the two O atoms of CO₂

(8) Tomita, M.; Irie, M.; Ukita, T. *Tetrahedron Lett.* **1968**, *47*, 4933–4936.

(9) Ryang, H.-S.; Foote, C. S. *J. Am. Chem. Soc.* **1979**, *101*, 6683–6687.

(10) Henderson, B. W.; Dougherty, T. J., Eds. *Photodynamic Therapy*; Marcel Dekker: New York, 1992; Ochsner, M. J. *Photochem. Photobiol.*, **B** **1997**, *39*, 1–18.

(11) Shen, H. R.; Spikes, J. D.; Kopeckova, P.; Kopecek, J. *J. Photochem. Photobiol.*, **B** **1996**, *35*, 213–219; Shen, H. R.; Spikes, J. D.; Kopeckova, P.; Kopecek, J. *J. Photochem. Photobiol.*, **B** **1996**, *34*, 203–210; Balasubramanian, D.; Du, X.; Zigler, J. S. *Photochem. Photobiol.* **1990**, *52*, 761–768.

(12) Shen, H. R.; Spikes, J. D.; Smith, C. J.; Kopecek, J. *J. Photochem. Photobiol.*, **A** **2000**, *130*, 1–6.

(13) Kang, P.; Foote, C. S. *J. Am. Chem. Soc.* **2002**, *124*, 4865–4873.

(14) Wasserman, H. H.; Wolff, M. S.; Stiller, K.; Saito, I.; Pickett, J. E. *Tetrahedron* **1981**, *37S1*, 191–200; Wasserman, H. H.; Vinick, F. J.; Chang, Y. C. *J. Am. Chem. Soc.* **1972**, *94*, 7180–7182; Wasserman, H. H.; Scheffer, J. R.; Cooper, J. C. *J. Am. Chem. Soc.* **1972**, *94*, 4991–4996; Wasserman, H. H. *Heterocycles* **1979**, *12*, 133–134; Lipshutz, B. H.; Morey, M. C. *J. Org. Chem.* **1983**, *48*, 3745–3750; Graziano, M. L.; Iesce, M. R.; Scarpati, R. *J. Chem. Soc., Chem. Commun.* **1979**, 7–8.

(15) Kang, P.; Foote, C. S. *Tetrahedron Lett.* **2000**, *41*, 9623–9626.

Table 1. CO₂ Formation in Photosensitized Oxidation of Imidazole Derivatives

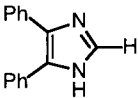
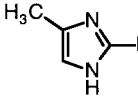
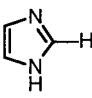
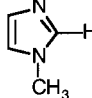
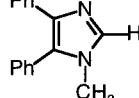
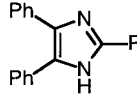
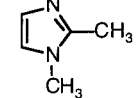
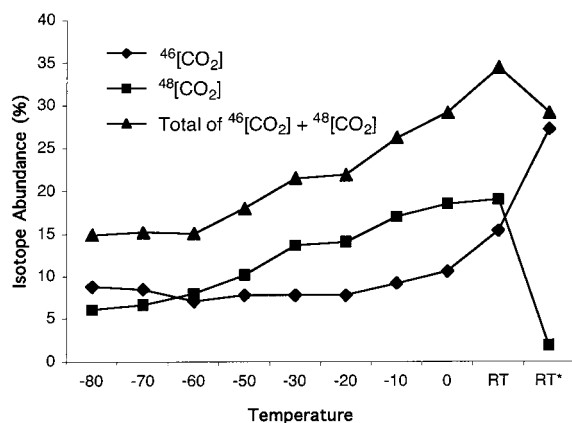
Entry	1	2	3	4	5	6	7
Substrate							
CO ₂ Formation	CO ₂	CO ₂	CO ₂	slight CO ₂	No CO ₂	No CO ₂	No CO ₂

Table 2. CO₂ Isotope Distribution in Photosensitized Oxidation of Imidazole Derivatives^a.

substrate		⁴⁴ [CO ₂]: ⁴⁵ [CO ₂]: ⁴⁶ [CO ₂]: ⁴⁸ [CO ₂]
4,5-diphenylimidazole ^c	exp ^b	100:1.19:1.87:2.08
	2-O ^{f,h}	100:1.10:0.44:3.97
	1-O ^g	100:1.98:7.94:0.16
4-methylimidazole ^d	exp ^b	100:1.21:3.04:2.06
	2-O ^{f,h}	100:1.10:0.50:5.44
	1-O ^g	100:2.10:10.88:0.29
imidazole ^e	exp ^b	100:1.16:2.66:2.66
	2-O ^{f,h}	100:1.10:0.46:5.99
	1-O ^g	100:2.02:11.98:0.36

^a Reaction mixture at rt after photolysis at -80 °C, after correction for CO₂ in air. ^b exp: experimental results. ^c Using ¹⁸O-enriched oxygen gas ³²[O₂]:³⁴[O₂]:³⁶[O₂] = 100:0.44:3.97. ^d Using ¹⁸O-enriched oxygen gas ³²[O₂]:³⁴[O₂]:³⁶[O₂] = 100:0.50:5.44. ^e Using ¹⁸O-enriched oxygen gas ³²[O₂]:³⁴[O₂]:³⁶[O₂] = 100:0.46:5.99. ^f 2-O: theoretical CO₂ isotope distribution using experimental O₂ isotope distribution based on the assumption that both O atoms of CO₂ are derived from one O₂ molecule. ^g 1-O: theoretical CO₂ isotope distribution using experimental O₂ isotope distribution based on the assumption that the O atoms of CO₂ are derived from two O₂ molecules. ^h According to the supplier, ³⁴[O₂] consists of two ¹⁷O. If ³⁴[O₂] consists of one ¹⁶O and one ¹⁸O 2-O would be the same as above and 1-O are not much different from the above. See Experimental Section for the details.

**Figure 1.** Change of ⁴⁶[CO₂] and ⁴⁸[CO₂] isotope abundance with temperature and time. Photooxidation of 4-methylimidazole in acetone. ¹⁸O enriched oxygen (³²[O₂]:³⁶[O₂] = 100:33.7) was used for the photooxidation. (*) Two days later.

came only from two different O₂ molecules, we would not expect such a significant amount of ⁴⁸[CO₂] (the highest calculated value for ⁴⁸[CO₂] is 0.36% for this scenario).

One probable reason that the ¹⁸O incorporation is lower than theoretical is that the initially formed ⁴⁸[CO₂] reacts with water, exchanging one ¹⁸O for ¹⁶O. The exchange rate should depend on temperature and should increase at higher temperatures. Figure 1 shows that the ⁴⁸[CO₂] isotope abundance continues to increase as the temperature of the reaction increases. The ⁴⁶[CO₂] isotope abundance does not change much until above

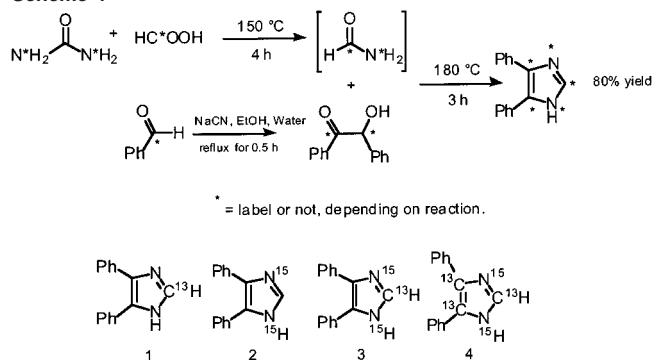
0 °C, where ⁴⁶[CO₂] increases much faster than ⁴⁸[CO₂], as a result of the exchange of ⁴⁸[CO₂] with water. These observations suggest that intermediates in the reaction decompose to form mainly ⁴⁸[CO₂] but not ⁴⁶[CO₂] as the temperature rises. After 2 days at room temperature, almost all ⁴⁸[CO₂] exchanges with water to form ⁴⁶[CO₂]. The ⁴⁶[CO₂] also exchanges with water at room temperature as the total isotope abundance decreases. The ¹⁸O experiments suggest that both O atoms of CO₂ in the photosensitized oxidation of imidazole derivatives originate mainly from one O₂ molecule but that both mechanisms contribute to the CO₂ formation. The increase in ⁴⁸[CO₂] with temperature implies that a low-temperature direct CO₂ formation pathway by a different mechanism exists.

Synthesis of ¹³C,¹⁵N-Labeled 4,5-Diphenylimidazole Derivatives. For unlabeled 4,5-diphenylimidazole, no transient intermediates could be detected at low temperature due to low solubility and low NMR sensitivity of the compound. To increase the NMR sensitivity we synthesized ¹³C,¹⁵N-labeled imidazoles. Various synthetic routes were evaluated.^{16–18} Because of the limitations on the availability of labeled starting material, most of the methods are not suitable. We chose a synthesis based on a procedure reported by Bakibaev et al.¹⁶ and Novelli.¹⁸ The synthesis involves first heating a mixture of ¹⁵N-urea and ¹³C-formic acid at 150 °C for 4 h. Benzoin was then introduced, and the reaction mixture was heated at 180 °C for 3 h. The product was suspended in water. After filtration, the powder was resuspended in 5% HCl and heated to 80–90 °C. The filtrate was treated with an excess of NH₃ to give pure 4,5-diphenylimidazole in 80% yield (Scheme 4). ¹³C-labeled benzoin was synthesized by coupling 2 mol of ¹³C benzaldehyde in the presence of NaCN (Scheme 4).

This synthetic method is versatile and selective with different, sometimes labeled, starting materials. We synthesized 2-¹³C-4,5-diphenylimidazole (**1**), 1,3-¹⁵N-4,5-diphenylimidazole (**2**), 2-¹³C-1,3-¹⁵N-4,5-diphenylimidazole (**3**), and 2,4,5-¹³C-1,3-¹⁵N-4,5-diphenylimidazole (**4**). The structures of labeled imidazoles were confirmed by ¹H NMR, ¹³C NMR, and high-resolution MS. In all four cases, the incorporation of isotope into imidazole is almost 100%. NMR couplings between these isotopes in the

- (16) Bakibaev, A. A.; Yagovkin, A. Y.; Filimonov, V. D. *Zh. Org. Khim.* **1991**, *27*, 1512–1519.
 (17) Bredereck, H.; Theilig, G. *Chem. Ber.* **1953**, *86*, 88–96; Bredereck, H.; Gompper, R.; Hayer, D. *Chem. Ber.* **1959**, *92*, 338–343; Chimishkyan, A. L.; Svetlova, L. P.; Leonova, T. V.; Gulyaev, N. D. *Zh. Obshch. Khim.* **1984**, *54*, 1477–1481; Cohen, L. A.; D'sa, A. J. *Heterocycl. Chem.* **1991**, *28*, 1819–1820; Grimmett, M. R. *Adv. Heterocycl. Chem.* **1970**, *12*, 103–183; Grimmett, M. R. In *Imidazoles and Their Benzo Derivatives (iii) Synthesis and Applications*; Katritzky, A. R., Rees, C. W., Potts, K. T., Eds.; Pergamon Press: New York, 1984; pp 457–497; Grimmett, M. R. In *Imidazoles*; Katritzky, A. R., Rees, C. W., Scriven, E. F. V., Eds.; Pergamon Press: New York, 1996; pp 79–220.
 (18) Novelli, A. *Anales Asoc. Quim. Argentina* **1952**, *40*, 112–114; *Chem. Abstr.* **1953**, *147*, 9321c.

Scheme 4



imidazole were observed. For example, we observed the splitting of the ^1H peak by ^{13}C ($J_{2\text{H}-2\text{C}} = 207.0$ Hz) and ^{15}N ($J_{2\text{H}-\text{N}} = 10.3$ Hz, $J_{1\text{H}-1\text{N}} = 96.4$ Hz), of the ^{13}C peak by ^1H ($J_{2\text{C}-2\text{H}} = 207.1$ Hz) and ^{15}N ($J_{2\text{C}-\text{N}} = 5.0$ Hz) in 2- ^{13}C -1,3- ^{15}N -diphenylimidazole, of the ^{15}N peak by ^1H ($J_{\text{N}1-\text{H}} = 97.2$ Hz) in 1,3- ^{15}N -diphenylimidazole, of the ^{13}C peak by an adjacent ^{13}C ($J_{\text{C}4-\text{C}5} = 71.9$ Hz) in 2,4,5- ^{13}C -1,3- ^{15}N -diphenylimidazole. The splitting of the ^{15}N peak by ^{13}C was not observed in the starting material but was detected in the products. These magnetic interactions are very useful in the identification of the transient intermediates in the photosensitized oxidation of imidazole (see next section).

Photosensitized Oxidation of Isotope-Labeled Imidazole Derivatives. To take advantage of the synthetic imidazoles with isotope labeling at various positions of the five-membered ring, we designed our experiments according to the following approach. First, the singly labeled 2- ^{13}C -diphenylimidazole was used in the photosensitized oxidation. The formation of the initial intermediate and its subsequent decomposition to other intermediates were followed by ^{13}C NMR. Since under our NMR acquisition conditions only the peaks of ^{13}C -labeled compounds show up in the carbon spectrum of the reaction mixture, each individual peak corresponds to one compound, which makes it easier to identify each transient intermediate and follow its changes. Using singly labeled 2- ^{13}C -diphenylimidazole also allows us to determine the conditions (solvent, temperature) under which each individual intermediate is stable. We could then choose the ideal conditions to study that intermediate in more detail. Next, we oxidized 2- ^{13}C -1,3- ^{15}N -4,5-diphenylimidazole, which provides additional spectroscopic information such as ^{15}N chemical shifts and ^{13}C - ^{15}N and ^{15}N - ^1H coupling constants. Finally, we used 2,4,5- ^{13}C -1,3- ^{15}N -4,5-diphenylimidazole, which yielded more spectroscopic data and allowed us to fully characterize these transient intermediates. This approach of using imidazoles with successive isotope labeling allowed us to obtain increasing structural information on the transient intermediates without increasing the complexity of interpreting the spectroscopic data.

Photosensitized oxidation of ^{13}C - or ^{15}N -labeled or ^{13}C , ^{15}N -labeled 4,5-diphenylimidazole was carried out in a 5-mm NMR tube at -100 °C with ca. 5×10^{-5} M of 2,9,16,23-tetra-*tert*-butyl-19*H*,31*H*-phthalocyanine as sensitizer and a Cemax 300-W xenon lamp as the light source. A chromium glass filter was used to cut off wavelengths below 547 nm. The starting material was dissolved in a solvent of acetone- d_6 and trichlorofluoromethane (1:5, ca. 0.04 M). After 30 min of photolysis, the NMR tube was transferred to a precooled NMR probe. Other

Table 3. Chemical Shifts of the Transient Intermediates.

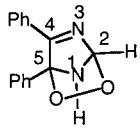
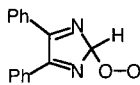
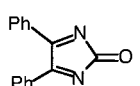
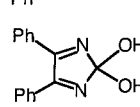
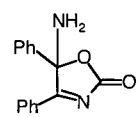
Transient Intermediates	^{13}C (ppm)			^{15}N (ppm)		^1H (ppm)	
	C2	C4	C5	N1	N3	C2-H	N1-H
	102.2	172.6	100.3	111.1	307.0	6.94	5.11
	117.5	167.0	167.0	356.6	356.6	6.82	N/A
	177.8	181.4	181.4	308.5	308.5	N/A	N/A
	127.3	162.9	162.9	364.2	364.2	N/A	N/A
	163.7	100.6	189.1	44.9	288.3	N/A	4.59

solvents such as acetone- d_6 and a mixture of dimethyl sulfoxide (DMSO- d_6) and CD_2Cl_2 were also used. Some intermediates are more stable in one solvent system than the other, which allowed us to make solutions enriched in one or another intermediate.

1. Characterization of Transient Intermediates. Photosensitized oxidation of 2- ^{13}C -4,5-diphenylimidazole at -100 °C gave one intermediate at -100 °C. There was only one ^{13}C (C2) peak in the reaction mixture with a chemical shift of 102.2 ppm (Tables 3 and 4). It is a tertiary carbon split into a doublet by a directly bonded hydrogen ($J_{\text{C}-\text{H}} = 194.1$ Hz). ^1H NMR of the first intermediate shows that the 2-H peak at 6.94 ppm was also split into a doublet ($J_{\text{H}-\text{C}} = 195.0$ Hz). HMQC also shows a cross-peak between the C2 peak and the 2-H peak (see Supporting Information). Introduction of 1,3- ^{15}N splits C2 into a doublet of doublets ($J_{\text{C}-\text{N}1} = 5.1$ Hz, $J_{\text{C}-\text{N}3} = 4.9$ Hz), which suggests C2 is bonded to two nonequivalent ^{15}N . The two ^{15}N peaks were also split into two doublets ($J_{\text{N}1-\text{C}} = 5.6$ Hz, $J_{\text{N}3-\text{C}} = 4.3$ Hz). The chemical shifts for the two ^{15}N are 111.1 ppm for N1 and 307.0 ppm for N3, which indicates that the N3 ^{15}N is an sp^2 nitrogen and the N1 ^{15}N is an sp^3 nitrogen. The N1 peak was split into a doublet ($J_{\text{N}1-\text{H}} = 70.0$ Hz) by one directly bonded hydrogen (^1H chemical shift 5.11 ppm). The corresponding splitting of ^1H by N1 ($J_{\text{H}-\text{N}1} = 69.7$ Hz) was also seen in the ^1H NMR of the intermediate. The ^1H - ^{15}N HMQC also confirmed the N1-H structure. The chemical shifts of C4 and C5 were obtained from the photosensitized oxidation of 2,4,5- ^{13}C -1,3- ^{15}N -4,5-diphenylimidazole. Both carbons are quaternary carbons. The chemical shift of C4 at 172.6 ppm suggests a C=N structure in the intermediate. The chemical shift of C5 is 100.3 ppm. C4 and C5 were split by each other into two doublets ($J_{\text{C}4-\text{C}5} = 46.2$ Hz). The chemical shifts of 102.2 ppm for C2 and 100.3 ppm for C5 are characteristic of sp^3 carbons directly bonded to two or more heteroatoms. On the basis of the above spectroscopic information, the initially formed intermediate is assigned to be a 2,5-endoperoxide **5**.

When the reaction mixture was warmed to -88 °C, the 2,5-endoperoxide began to decompose, and several other intermediates were formed. (Tables 3 and 4) ^1H NMR of the second intermediate showed a hydrogen at 11.85 ppm, consistent with an OOH proton. The chemical shift of C2 is 117.5 ppm, which

Table 4. Coupling Constants of the Transient Intermediates

Transient Intermediates	J_{C2-H} (Hz)	J_{H-C2} (Hz)	J_{N1-H} (Hz)	J_{H-N1} (Hz)	J_{C2-N} (Hz)	J_{N-C2} (Hz)	J_{C4-C5} (Hz)	
	5	194.1	195.0	70.0	69.7	4.9, 5.1	4.3, 5.6	46.2
	6	161.2	160.6	N/A	N/A	4.7	4.7	N/A
	7	N/A	N/A	N/A	N/A	6.5	6.5	N/A
	8	N/A	N/A	N/A	N/A	1.5	N/A	N/A
	9	N/A	N/A	74.0	74.2	2.3	2.3	39.0

is split into a doublet by a directly bonded hydrogen at 6.82 ppm ($J_{C2-H} = 161.2$ Hz). The hydrogen at 6.82 ppm is a doublet ($J_{H-C2} = 160.6$ Hz). $^1H-^{13}C$ HMQC also showed the connectivity of this hydrogen to C2 (see Supporting Information). The C2 peak becomes a triplet in the presence of $^{15}N1$ and $^{15}N3$ ($J_{C2-N} = 4.7$ Hz), which shows that C2 is connected to two equivalent N. The equivalence of N1 and N3 is confirmed by the identical chemical shift of $^{15}N1$ and $^{15}N3$ (both 356.6 ppm). The ^{15}N peak was also split into a doublet by C2 ($J_{N-C2} = 4.7$ Hz). The chemical shifts of C4 and C5 are also identical (167.0 ppm), showing two C=N structures in the second intermediate. The ^{13}C intensity ratio of 167.0 ppm (C4 and C5) to 117.5 ppm (C2) is 2:1. No N1-H signal was visible in the 1H NMR of this intermediate. The chemical shift of C2 (117.5 ppm) suggests an sp^3 carbon connected to three heteroatoms. We assigned the second intermediate as hydroperoxide **6** with C_{2v} symmetry.

The third intermediate was formed as the temperature was raised to -80 °C. It has a symmetry plane, as evidenced by the identical chemical shifts of C4 and C5 (181.4 ppm) and of N1 and N3 (308.5 ppm). (Tables 3 and 4) These chemical shifts show there are two C=N structures in the third intermediate. The chemical shift of C2 is 177.8 ppm, a quaternary carbon, split into a triplet by $^{15}N1$ and $^{15}N3$ ($J_{C2-N} = 6.5$ Hz). The corresponding splittings were also seen in $^{15}N1$ and $^{15}N3$ ($J_{N-C2} = 6.5$ Hz). Both 2-H and N1-H signals were absent in the third intermediate. The chemical shift of 177.8 ppm suggests a carbonyl carbon for C2. On the basis of the above information, the structure of the third intermediate is assigned to be **7**.

The fourth intermediate appeared as the reaction was warmed to -80 °C. It is also symmetrical, since the chemical shifts for C4 and C5 are at 162.9 ppm and those for N1 and N3 are at 364.2 ppm (Table 3, Table 4). The chemical shifts also suggest two C=N structures in this intermediate. C2, a quaternary carbon at 127.3 ppm, was split into a triplet by $^{15}N1$ and $^{15}N3$ ($J_{C2-N} = 1.5$ Hz), showing the connectivity of C2 to both $^{15}N1$ and $^{15}N3$. The C2 chemical shift is characteristic of an sp^3 carbon directly bonded to four heteroatoms. On the basis of the above spectroscopic information either a dioxirane or a diol from the ring opening of dioxirane would be possible structures

for the intermediate. However, the dioxirane would have to have sp^3 N-H nitrogens to be at the correct oxidation state, and the chemical shifts are in the range for sp^2 nitrogen and are unsplit by hydrogen. A $^1H-^{13}C$ HMBC experiment showed a cross-peak between C2 and two hydrogens at 8.25 ppm (see Supporting Information). This hydrogen was not directly bonded to either a carbon or a nitrogen, as no cross-peaks were found in either $^1H-^{13}C$ HMQC or $^1H-^{15}N$ HMQC. This hydrogen was thus assigned to be OH. From the spectroscopic evidence, the fourth intermediate is diol **8**.

The fifth intermediate appeared at around -60 °C. It is not symmetrical. The chemical shift of C2 is 163.7 ppm (Tables 3 and 4). It is a quaternary carbon, split into a doublet by either $^{15}N1$ or $^{15}N3$ ($J_{C2-N} = 2.3$ Hz), indicating that one C2-N bond is broken in the fifth intermediate. The corresponding splitting of ^{15}N by C2 is found only in N3 (chemical shift at 288.2 ppm, $J_{N3-C2} = 2.3$ Hz) but not in N1 (chemical shift at 44.9 ppm). The chemical shifts of N3 and C5 (189.1 ppm) show a C=N double bond in the intermediate. N1 is an amino group, since it is a triplet split by two bonded hydrogens ($J_{N1-H} = 74.0$ Hz). N1-H has a chemical shift of 4.59 ppm and is a doublet ($J_{H-N1} = 74.2$ Hz). The chemical shift of C4 (100.6 ppm) is characteristic of an sp^3 carbon connected to two heteroatoms, which indicates C4 is bonded to an oxygen and the N1 nitrogen. C4 and C5 are split by each other into two doublets ($J_{C4-C5} = 39.0$ Hz). The above spectroscopic information suggests that the five-membered imidazole ring was opened and reclosed to form the fifth intermediate, assigned to be **9**.

2. Transformation of One Intermediate to Another. The transformation of one intermediate to another was followed by quantitative analysis of C2 ^{13}C NMR peak changes with temperature and time. When the reaction mixture was warmed to 253 K (-20 °C), only two intermediates were left, **7** and **9**. Further warming from 253 to 273 K (0 °C) caused the **9** (163.7 ppm) peak to decrease and that of CO_2 (124.0 ppm) to increase. Intermediate **9** decomposed completely to CO_2 at 273 K (Figure 2, panel A). As a check, the total intensity of **9** and CO_2 remained unchanged. The absorption of **7** (177.8 ppm) did not change during this process. This analysis clearly shows that most

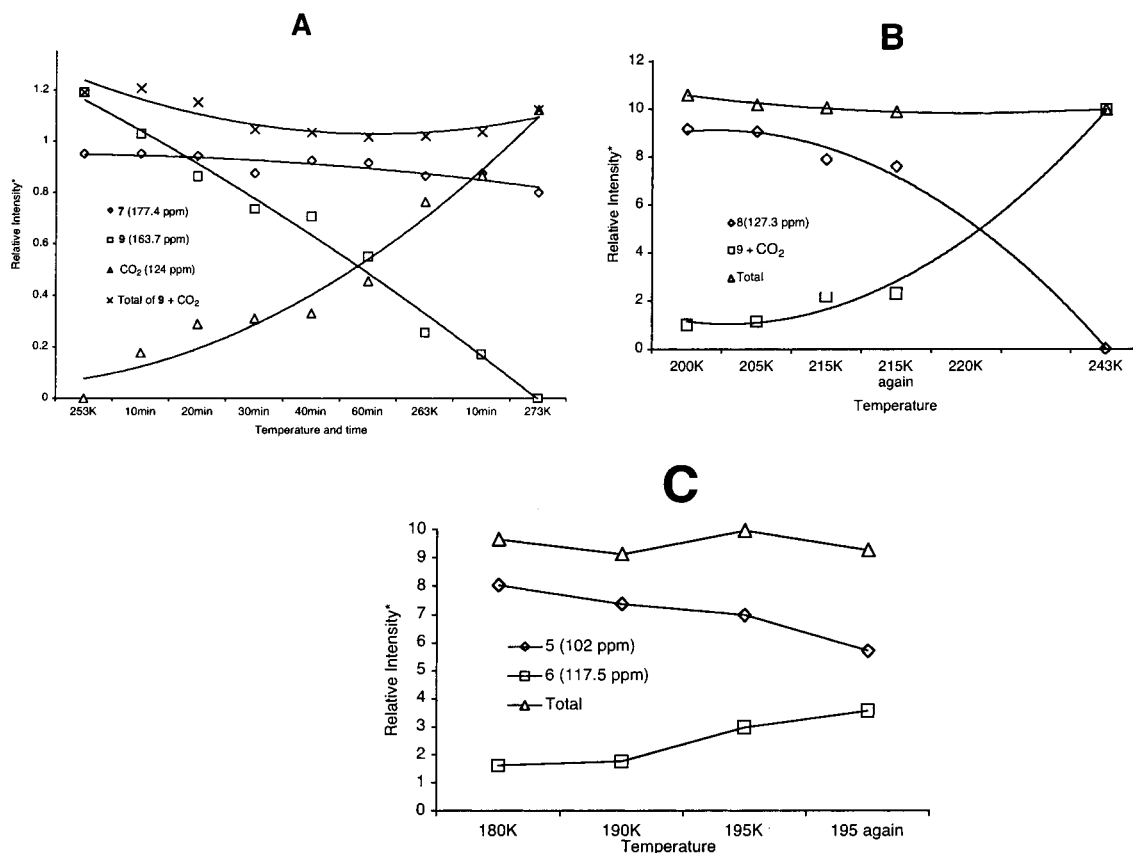


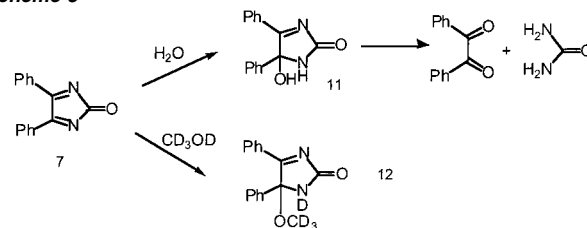
Figure 2. Correlation of decomposition of one intermediate to the formation of another intermediate. (Panel A) Decomposition of intermediate **9** to CO₂ and 1,2-diphenylethanediiimine. (Panel B) Decomposition of intermediate **8** to form **9**. (Panel C) Decomposition of endoperoxide **5** to hydroperoxide **6**. (*) The reference of the relative intensity is acetone-*d*₆ at 206 ppm.

of the CO₂ originates from **9**. Intermediate **7** is not involved in CO₂ formation. **9** decomposes to CO₂ and another product, 1,2-diphenylethanediiimine (benzil diimine), **10** (Scheme 8). A low-temperature FAB/MS spectrum shows the molecular ion for **9** (m/z 253.1 [M + H]⁺) and for benzil diimine (m/z 209.1 [M + H]⁺). Benzil diimine was fully characterized by ¹³C, ¹H, ¹⁵N NMR and ¹H–¹⁵N HMQC (see Experimental Section for details). Benzil diimine is not stable at room temperature and decomposes to a complex mixture, probably via hydrolysis of the diimine and subsequent reactions between these hydrolyzed products. However, we were able to isolate benzil from the reaction mixture at room temperature by column chromatography. The complexity of the decomposition of benzil diimine from the photosensitized oxidation of 4,5-diphenylimidazole may explain why the isolated yields of product from photosensitized oxidation of 2-H imidazoles are usually low.

Intermediate **7** decomposed as we warmed the reaction mixture to room temperature. **11** was formed from attack of adventitious water on intermediate **7**. **11** is not stable at room temperature and decomposes to benzil and urea. When we added methanol at low temperature after the photosensitized oxidation and warmed it to room temperature, we detected methanol adduct **12** (Scheme 5) and the water adduct (**11**) was suppressed.

By following the ¹³C peak changes of the reaction mixture from 200 K (–73 °C) to 243 K (–30 °C), we found that decomposition of intermediate **8** (127.3 ppm) leads to the formation of intermediate **9** (163.7 ppm). Figure 2 panel B shows that the intensity decrease of **8** was accompanied by an increase of those of **9** and CO₂. The total intensities of the three

Scheme 5

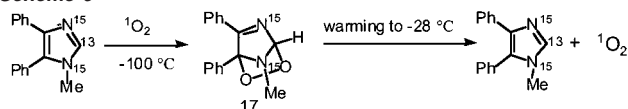


compounds did not change. Since we have shown that CO₂ is derived from **9**, it is clear that the decomposition of **8** leads to **9**, which further decomposes to form CO₂.

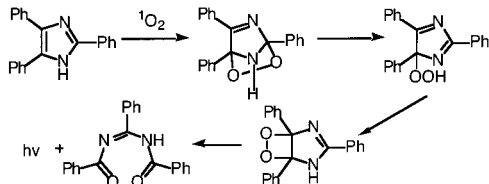
Quantitative analysis of the NMR of the reaction mixture from 180 K (–93 °C) to 195 K (–78 °C) revealed that the endoperoxide decomposed to form the intermediate with C-2 at 117.5 ppm. Over this temperature range, only these two intermediates exist in the reaction mixture. Figure 2 panel C shows that as the 102.2 ppm peak decreases, the 117.5 ppm peak increases, and the total intensity remains constant.

The lifetimes of the intermediates depend on the solvent system used. When the photosensitized oxidation was done in a mixture of CD₂Cl₂ and DMSO-*d*₆, a predominant amount of intermediate **8** and only a very small amount of intermediate **6** were formed. **8** was more stable in a mixture of CD₂Cl₂ and DMSO-*d*₆ than in either acetone-*d*₆ or CD₂Cl₂. When the reaction was done in acetone-*d*₆, we saw a large amount of **6** and a very small amount of **8**. The polarity of the solvent or the water impurity in DMSO-*d*₆ may be responsible for these differences.

Scheme 6



Scheme 7



Photosensitized Oxidation of *N*-Methyl-4,5-diphenylimidazole. The decomposition of the endoperoxide is triggered by the rearrangement of the N1-H, since this peak disappeared as the endoperoxide decomposed. This observation suggested that substitution of the N-H by *N*-methyl would stabilize the endoperoxide. The photosensitized oxidations of *N*-methyl-4,5-diphenylimidazole, *N*-methyl-1,3-¹⁵N-4,5-diphenylimidazole, and *N*-methyl-2-¹³C-1,3-¹⁵N-4,5-diphenylimidazole were carried out under similar conditions. The endoperoxide **17** (see Experimental Section for characterization) is much more stable than the unmethylated endoperoxide and does not decompose until -28 °C. The decomposition of the endoperoxide regenerated the starting material (Scheme 6). Adding a methyl to the 1N position of the imidazole totally changes the reaction pathway of the endoperoxide rearrangement, which suggests that proton transfer from the N-H is much more facile than the extrusion of oxygen.⁹

Discussion

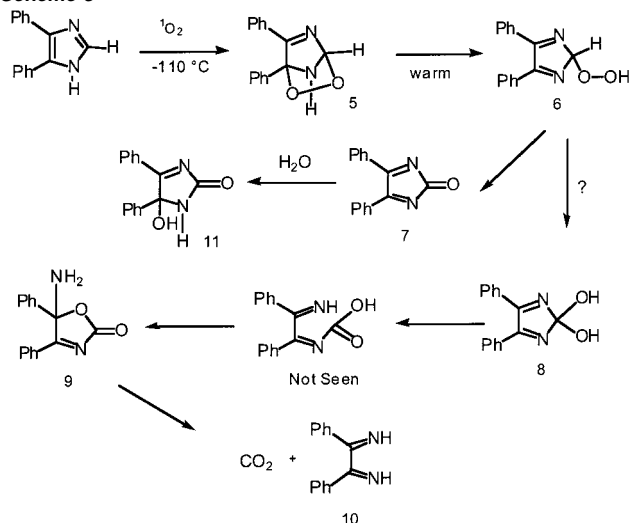
On the basis of the structures of the various intermediates and the information on transformation of one intermediate to another, we propose a mechanism for the photosensitized oxidation of 4,5-diphenylimidazole (Scheme 8). Singlet oxygen reacts with 4,5-diphenylimidazole via a [4 + 2] cycloaddition to form the initial product 2,5-endoperoxide **5**. Upon warming to 185 K (-88 °C), the 2,5-endoperoxide decomposes to form hydroperoxide **6**.

A hydroperoxide of 2,4,5-triphenylimidazole (lophine) was shown to be the precursor to the light emitter for the chemiluminescence in the reaction of lophine with air in the presence of base.⁷ The hydroperoxide was also prepared from the photosensitized oxidation of lophine in the presence of methylene blue and oxygen and underwent decomposition with chemiluminescence through the dioxetane⁶ (Scheme 7). We did not observe dioxetane formation in the decomposition of hydroperoxide **6**, which indicates that **6** decomposes by a different reaction pathway. Another difference is the position of the peroxidic group. In lophine hydroperoxide the peroxidic group is on the C4 position of the imidazole ring, whereas in **6** the peroxidic group is on the C2 position.

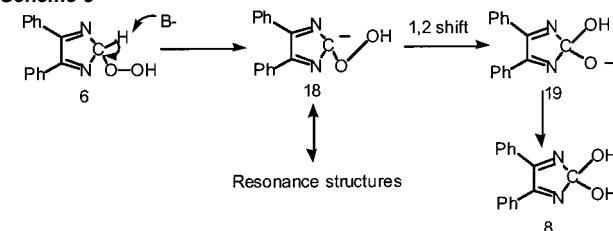
The hydroperoxide in one pathway loses water to form **7**, which is hydrolyzed to **11**. In another pathway, the hydroperoxide **6** decomposes to diol **8**. As evidence for this suggestion, the 2,5-endoperoxide decomposes quantitatively to form the hydroperoxide before the appearance of other intermediates, and the hydroperoxide always decomposes before the diol.

The decomposition of the hydroperoxide to diol is unprecipitated. The diol does not come from addition of water to **7**

Scheme 8



Scheme 9



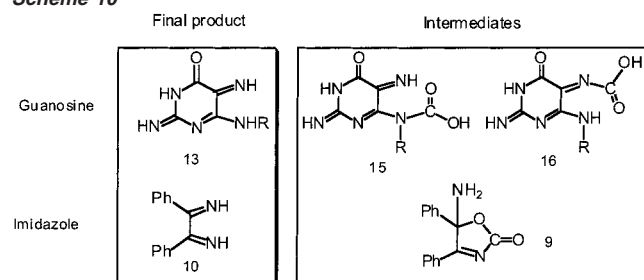
since **7** is not on that pathway, and this reaction would not explain the oxygen isotope composition of the CO₂. A dioxirane intermediate was suggested in a previous study of photooxidation of an 8-¹³C guanosine derivative,¹³ however there is no evidence for its involvement in this reaction. We cannot provide a completely satisfactory mechanism at present. One possibility is shown in Scheme 9. Cleavage of the C2-H bond in the presence of a trace amount of base gives carbanion **18**, which can be stabilized by several resonance structures and the 6- π -electron aromatic ring system. 1,2-Shift of the carbanion results in **19**. Protonation of **19** gives diol **8**. This mechanism is consistent with the fact that the two oxygen atoms of CO₂ come from one molecular oxygen. Dehydration of **8** to **7** would be inhibited by the fact that **7** is a cyclopentadienone.

The rearrangement of the diol to **9** probably proceeds via the formation of a ring-opened carbamate intermediate that recloses the ring to form **9**, which finally decomposes to CO₂ and benzil diimine.

The mechanistic studies of photosensitized oxidation of guanosine and 4,5-diphenylimidazole show many similarities. (1) In both reactions, CO₂ is generated, and the carbon of CO₂ originates from the C2 of the five-membered imidazole ring. The oxygen atoms of CO₂ come from one molecule of oxygen. (2) CO₂ was only observed in the photosensitized oxidation of the 2-H imidazoles. There was no CO₂ formation in the photosensitized oxidation of 2-substituted imidazoles such as 2-methylimidazole. Substitution of the 8-H of guanosine by a methyl group did not yield any CO₂ in the photosensitized oxidation.¹⁹ (3) The final products from reactions in organic solvent both have an imidazole ring-opened diimine structure or its tautomer: benzil diimine **10** in the reaction of imidazole

(19) Sheu, C.; Foote, C. S. *J. Am. Chem. Soc.* **1993**, *115*, 10446–10447.

Scheme 10

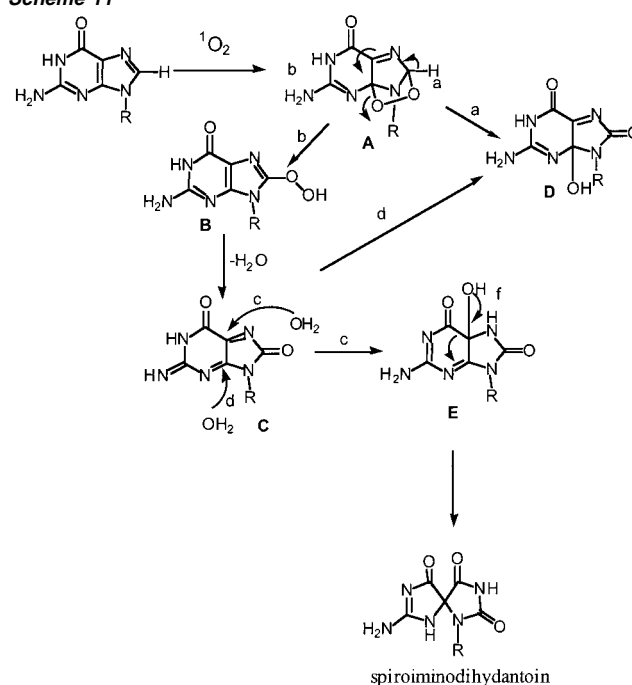


and an imidazole ring-opened product **13** in the reaction of guanosine (Scheme 10). (4) The intermediates that decompose to CO_2 in the photosensitized oxidation of guanosine and in that of imidazole both have carbamate structures (**15** and **16** in guanosine and **9** in imidazole, Scheme 10) Whether the carbamic acid intermediates in the reaction of guanosine is the ring-opened or -closed form is not clear at present. (5) An endoperoxide was proposed to be the initially formed product in the photosensitized oxidation of guanosine, and the endoperoxide was directly detected in the reaction of imidazole. These similarities suggest that the mechanism of photosensitized oxidation of guanosine in nonpolar organic solvent probably proceeds similarly to that of 4,5-diphenylimidazole in part.

A major product from photosensitized oxidation of guanosine in nonpolar organic solvent is **13**, whereas the main products from photosensitized oxidation of 2'-deoxyguanosine in aqueous medium are the diastereomers of spiroiminodihydantoin.^{20–22} In both cases, the yields are less than 50%. The overall reaction is analogous to the photosensitized oxidation of 4,5-diphenylimidazole, where the common intermediate is the 2,5-endoperoxide and two reaction pathways lead to two different products: benzil diimine and 4,5-diphenyl-4-hydroxyimidazol-2-one. The reaction pathway to benzil diimine is probably similar to the pathway to **13**; there are many similarities between the two pathways. If the reaction pathway to 4,5-diphenyl-4-hydroxyimidazol-2-one is the same in the guanosine reaction, 4,8-dihydro-4-hydroxy-8-oxo-guanosine (D, Scheme 11) or 5,8-dihydro-5-hydroxy-8-oxo-guanosine (E, Scheme 11) or both would be formed. E has been proposed to be the intermediate in both the peroxyxynitrite oxidation²² and in the one-electron oxidation²¹ of 7,8-dihydro-8-oxo-guanosine, which contracts the six-membered ring to the spiroiminodihydantoin. D and E can be formed by water attacking the $\text{C}=\text{N}$ at 4 (pathway d) or 5 (pathway c) position of an intermediate C which has a structure similar to that of **7**. D can also be formed directly from the ring opening of the endoperoxide A (pathway a) as previously proposed by Cadet.

An important difference between the imidazole and guanosine oxidations is that in imidazole, the labile proton is the N1-H, whereas in the guanosine, it is the C8-H; this leads to the major difference in the first ring-opened intermediate (B in guanosine), since, like the *N*-methyl derivatives of histidine, the endoperoxide from the 8-methyl derivative of guanosine is relatively stable and only loses oxygen.¹⁹

Scheme 11



Conclusions

A detailed mechanistic study of the photosensitized oxidation of isotope-labeled imidazole derivatives was carried out, and a mechanism was proposed on the basis of this study. Singlet oxygen initially reacts with 4,5-diphenylimidazole via a [4 + 2] cycloaddition to form a 2,5-endoperoxide. Upon warming, the 2,5-endoperoxide decomposes to form the hydroperoxide which decomposes in two pathways. In one pathway, the hydroperoxide loses water to form **7**, which is hydrolyzed to **11**. In another pathway, the hydroperoxide decomposes to diol **8**. The diol rearranges to **9** by opening and reclosing the five-membered ring. **9** decomposes to CO_2 and benzil diimine **10**. A labile NH in the imidazole is required for the decomposition of the initially formed endoperoxide. Otherwise the endoperoxide decomposes back to starting material. A comparison with the reaction of guanosine derivatives in organic solvent shows many similarities between the two reactions such as the structures of the final relatively stable products, structures of carbamate intermediates that decompose to CO_2 and so forth, suggesting that the two reactions share a similar reaction mechanism with singlet oxygen.

Experimental Section

^1H NMR and ^{13}C NMR spectra were recorded on Bruker ARX-400, ARX-500, and Avance 500 spectrometers. Low-temperature NMR spectra were taken in a pre-cooled probe maintained at the desired temperature. The solvents for low-temperature NMR were acetone- d_6 , a mixture of DMSO- d_6 and CD_2Cl_2 , and CCl_3F with several drops of acetone- d_6 added as locking solvent. GC/MS spectra were recorded on a HP G1800 A GCD with HP-5 GC column (crosslinked 5% PH ME siloxane, 30 m \times 0.25 mm \times 0.25 μm). Positive ion FAB mass spectra were collected on a VG ZAB-SE reverse geometry, extended mass range, magnetic sector mass spectrometer. Thin-layer chromatography (TLC) was done using either DC-Fertigplatten Kieselgel 60F254 or DC-Plastikfolien Kieselgel 60 F254 from E. Merck. Column chromatography was performed on silica gel 60, 70–230 mesh or 230–400 mesh from E. Merck.

(20) Ravanat, J. L.; Cadet, J. *Chem. Res. Toxicol.* **1995**, *8*, 379–388; Luo, W. C.; Müller, J. G.; Rachlin, E. M.; Burrows, C. J. *Org. Lett.* **2000**, *2*, 613–616; Adam, W. Personal communication, 2001.

(21) Luo, W. C.; Müller, J. G.; Rachlin, E. M.; Burrows, C. J. *Chem. Res. Toxicol.* **2001**, 927–938.

(22) Niles, J. C.; Wishnok, J. S.; Tannenbaum, S. R. *Org. Lett.* **2001**, *3*, 963–966.

Materials. ^{13}C -Carbonyl benzaldehyde, urea- $^{15}\text{N}_2$, and formic acid- ^{13}C were from Isotec Inc. Deuterated solvents were from Cambridge Isotope Laboratory. NaCN, HCl, NH_4OH , K_2CO_3 were from Fisher Scientific. Dimethyl carbonate, 18-crown-6-imidazole, 1-methylimidazole, 1,2-methylimidazole, 4-methylimidazole, and 2,4,5-triphenylimidazole were from Aldrich. 4,5-diphenylimidazole was from Lancaster.

Preparation of 1,2- ^{13}C -Benzoin. To 0.65 mL of ethanol (95%), 0.5 mL of water, and 0.5 g of NaCN in a 10-mL round-bottomed flask was added 0.5 g of ^{13}C -Carbonyl benzaldehyde (0.5 g). The reaction mixture was heated to boiling (90–95 °C). After 0.5 h reaction, the solution was cooled with an ice bath and filtered with suction. The resulting solid product was washed with water and dried to give 1,2- ^{13}C -benzoin 0.33 g (66% yield).

^1H NMR (CDCl_3 , δ 7.32 ppm) 7.89 (m, 4H, phenyl ortho-H), 7.49 (m, 2H, phenyl para-H), 7.39 (m, 4H, phenyl meta-H), 5.93 (dd, $^1J_{\text{C-H}} = 146.7$ Hz, $^3J_{\text{C-H}} = 2.91$ Hz, 1H, HO–C–H). ^{13}C NMR (CDCl_3 , δ 77.0 ppm) 198.9 (d, 1C, C=O, $J_{\text{C-C}} = 39.1$ Hz), 76.2 (dd, 1C, C–OH, $J_{\text{C-H}} = 147.3$ Hz, $J_{\text{C-C}} = 39.1$ Hz). HRMS-EI (m/z): 214.0899 (Calculated 214.0904).

General Procedure for Preparation of Isotope-Labeled 4,5-Diphenylimidazole. A mixture of urea (1.2 g) and formic acid (1.2 g 95%) in a 10-mL round-bottomed flask was heated in an oil bath at 150 °C for 4 h. After cooling it down to 70 °C, 1.05 g of benzoin was added, and the reaction mixture was heated at 180 °C for 3 h. The reaction mixture was poured into 70 mL of water and stirred vigorously to dissolve the gummy product. The resulting powder was filtered, washed with water, and suspended in 5% HCl (50 mL). The solution was heated to 80–90 °C and filtered hot, and the acidic filtrate was treated with an excess of NH_4OH to form a white precipitate, which was filtered and dried to give 0.86 g of 4,5-diphenylimidazole (80% yield based on starting benzoin).

2- ^{13}C -4,5-Diphenylimidazole, 1. The starting materials were urea, formic acid- ^{13}C , and benzoin. ^1H NMR (CDCl_3 , δ 7.32 ppm) 7.98, 7.46 (d, 1H, C2–H, $J_{\text{C2-H}} = 206.9$ Hz), 7.51 (m, 4H, phenyl), 7.32 (m, 6H, phenyl), 3.36 (s, broad, 1H, N1–H). ^{13}C NMR (acetone- d_6 , δ 206.0 ppm) 134.6 (d, 1C, C2, $J_{\text{C2-H}} = 207.0$ Hz), 127.8, 127.2, 125.5 (phenyl). HRMS-EI (m/z): 221.1032 (Calculated 221.1034).

1,3- ^{15}N -4,5-Diphenylimidazole, 2. The starting materials were urea- $^{15}\text{N}_2$, formic acid, and benzoin. ^1H NMR (acetone- d_6 , δ 2.07 ppm) 7.76 (t, 1H, C2–H, $J_{\text{N-H}} = 10.3$ Hz), 7.55 (m, 4H, phenyl), 7.27–7.36 (m, 6H, phenyl), 5.13 (d, 1H, N1–H, $J_{\text{H-N1}} = 88.4$ Hz). ^{15}N NMR (DMSO- d_6 , urea- $^{15}\text{N}_2$ δ 73.4 ppm) 261.5 (1N, N3), 170.1 (1N, N1, $J_{\text{N1-H}} = 97.2$ Hz). HRMS-EI (m/z): 222.0939 (Calculated 222.0941).

2- ^{13}C -1,3- ^{15}N -4,5-Diphenylimidazole, 3. The starting materials were urea- $^{15}\text{N}_2$, formic acid- ^{13}C , and benzoin. ^1H NMR (DMSO- d_6 , δ 2.49 ppm) 12.46 (d, 1H, N1–H, $J_{\text{N1-H}} = 78.9$ Hz), 7.96, 7.55 (dt, 1H, C2–H, $J_{\text{C2-H}} = 206.7$ Hz, $J_{\text{N-H}} = 10.2$ Hz), 7.43 (m, 4H, phenyl), 7.32, 7.25 (m, 6H, phenyl). ^{13}C NMR (DMSO- d_6 , δ 39.5 ppm, H-decoupled) 135.6 (t, 1C, C2, $J_{\text{C2-N}} = 5.0$ Hz), 128.5, 127.5, 126.4 (phenyl). ^{15}N NMR (DMSO- d_6 , urea- $^{15}\text{N}_2$ δ 73.4 ppm) 263.6 (1N, N3), 170.9 (1N, N1). HRMS-EI (m/z): 223.0968 (Calculated 223.0976).

2,4,5- ^{13}C -1,3- ^{15}N -4,5-Diphenylimidazole, 4. The starting materials were urea- $^{15}\text{N}_2$, formic acid- ^{13}C , and 1,2- ^{13}C -benzoin. ^1H NMR (DMSO- d_6 , δ 2.50 ppm) 12.28, 12.09 (d, 1H, N1–H, $J_{\text{N1-H}} = 93.0$ Hz), 7.68 (d, 1H, C2–H, $J_{\text{C2-H}} = 206.9$ Hz), 7.53–7.25 (m, 10H, phenyl H). ^{13}C NMR (DMSO- d_6 , δ 39.5 ppm) 134.6 (d, 1C, C2, $J_{\text{C2-H}} = 207.0$ Hz), 135.9 (d, 1C, C5, $J_{\text{C4-C5}} = 91.4$ Hz), 126.1 (d, 1C, C4, $J_{\text{C5-C4}} = 91.0$ Hz). ^{15}N NMR (DMSO- d_6 , urea- $^{15}\text{N}_2$ δ 73.4 ppm) 261.7 (1N, N3), 170.1 (1N, N1). HRMS-EI (m/z): 225.1042 (Calculated 225.1042).

Preparation of *N*-Methyl-4,5-diphenylimidazole. A mixture of 1.0 g of K_2CO_3 , 0.2 g of 4,5-diphenylimidazole, 2.5 mL of dimethyl carbonate, and 12 mg of 18-crown-6 in a 10-mL round-bottomed flask was heated at 100 °C for 10 h. Dimethyl carbonate was removed by evaporation under vacuum. The residue was extracted with ether, and rotary evaporation gave 0.18 g of *N*-methyl-4,5-diphenylimidazole (85% yield).

^1H NMR (CDCl_3 , δ 7.31 ppm) 7.62 (s, 1 H, C2–H), 7.58–7.17 (m, 10 H, phenyl), 3.54 (s, 3H, NCH_3). ^{13}C NMR (CDCl_3 , δ 77.0 ppm) 138.28 (C5), 137.39 (C2), 134.64 (C4), 130.64, 130.57, 128.96, 128.88, 128.56, 128.08, 126.58, 126.27, (phenyl), 31.11 (NCH_3).

***N*-Methyl-2- ^{13}C -1,3- ^{15}N -4,5-diphenylimidazole.** The starting material was 1,3- ^{15}N -4,5-diphenylimidazole. ^1H NMR (CDCl_3 , δ 7.33 ppm) 7.58 (dd, 1 H, C2–H, $J_{\text{C2-H}} = 206.0$ Hz, $J_{\text{N1-H}} = 11.2$ Hz, $J_{\text{N3-H}} = 8.1$ Hz), 7.54–7.17 (m, 10 H, phenyl), 3.54 (s, 3H, NCH_3). ^{13}C NMR (CDCl_3 , δ 77.0 ppm) 138.28 (C5), 137.39 (ddd, C2, $J_{\text{C-H}} = 206.0$ Hz, $J_{\text{C-N1}} = 11.4$ Hz, $J_{\text{C-N3}} = 0.5$ Hz), 134.64 (C4), 130.69, 129.01, 128.62, 128.14, 126.64, 126.62, 126.34, 32.22 (dd, $J_{\text{C-N1}} = 11.1$, $J_{\text{C-N3}} = 1.9$ Hz). ^{15}N NMR (acetone- d_6 , urea- $^{15}\text{N}_2$ δ 73.4 ppm) 252.7 (N3), 162.8 (d, N1, $J_{\text{N-C}} = 11.7$ Hz). HRMS-EI (m/z): 237.1126 (Calculated 237.1132).

Photosensitized Oxidation of Imidazole Derivatives. Photosensitized oxidations of ca. 4 mg of isotope-labeled 4,5-diphenylimidazole derivative were carried out in a 5-mm NMR tube at -100 °C with ca. 5×10^{-5} M of 2,9,16,23-tetra-*tert*-butyl-19*H*,31*H*-phthalocyanine as sensitizer and a Cermax 300-W xenon lamp as the light source. A chromium glass filter was used to cut off wavelengths below 547 nm. The starting material was dissolved in a solvent of acetone- d_6 and trichlorofluoromethane (1:5). Dry O_2 was bubbled into the solution continuously. After 30 min of photolysis, the NMR tube was transferred to a precooled NMR probe. Other solvents such as acetone- d_6 and a mixture of dimethyl sulfoxide (DMSO- d_6) and CD_2Cl_2 were also used in the reaction. Low-temperature NMR spectra were taken on the Bruker ARX 500 or Avance 500. The temperature range was -100 °C to room temperature. Photooxidations were also carried out in acetone- d_6 , and a mixture of CD_2Cl_2 and DMSO- d_6 at -80 °C.

Quantitative analysis of the ^{13}C NMR spectrum was carried out by integrating ^1H -coupled ^{13}C NMR peaks. A control experiment showed that intensity of CO_2 did not change much from -90 to -10 °C, which suggests that CO_2 was still dissolved in the solvent. Since we were following the same carbons in the reaction mixture, integrating ^1H -coupled ^{13}C NMR peaks can provide reliable information about concentration changes in the reaction mixture.

Intermediate 5: ^1H NMR (acetone- d_3 , δ 2.06 ppm) 6.94 (d, 1 H, C2–H, $J_{\text{C2-H}} = 195.0$ Hz), 7.77–7.34 (m, 10 H, phenyl), 5.11 (d, 1 H, N1–H, $J_{\text{N1-H}} = 69.7$ Hz). ^{13}C NMR (acetone- d_3 , δ 206.0 ppm) 102.2 (ddd, C2, $J_{\text{C-H}} = 194.1$ Hz, $J_{\text{C-N1}} = 5.1$ Hz, $J_{\text{C-N3}} = 4.9$ Hz), 100.3 (d, C5, $J_{\text{C4-C5}} = 46.2$ Hz), 172.6 (d, C4, $J_{\text{C5-C4}} = 46.2$ Hz). ^{15}N NMR (urea- $^{15}\text{N}_2$ δ 73.4 ppm) 307.0 (d, N3, $J_{\text{N-C}} = 5.6$ Hz), 111.1 (dd, N1, $J_{\text{N1-H}} = 70.0$ Hz, $J_{\text{N3-C}} = 4.3$ Hz).

Intermediate 6: ^1H NMR (acetone- d_3 , δ 2.06 ppm) 11.85 (s, OOH), 6.82 (d, 1 H, C2–H, $J_{\text{C2-H}} = 160.6$ Hz), 7.77–7.34 (m, 10 H, phenyl). ^{13}C NMR (acetone- d_3 , δ 206.0 ppm) 117.5 (dt, C2, $J_{\text{C-H}} = 161.2$ Hz, $J_{\text{C-N}} = 4.7$ Hz), 167.0 (s, C4, C5). ^{15}N NMR (urea- $^{15}\text{N}_2$ δ 73.4 ppm) 356.6 (d, N1, N3, $J_{\text{N-C}} = 4.7$ Hz).

Intermediate 7: ^1H NMR (acetone- d_3 , δ 2.06 ppm) 7.77–7.34 (m, 10 H, phenyl). ^{13}C NMR (acetone- d_3 , δ 206.0 ppm) 177.8 (t, C2, $J_{\text{C-N}} = 6.5$ Hz), 181.4 (s, C4, C5). ^{15}N NMR (urea- $^{15}\text{N}_2$ δ 73.4 ppm) 308.5 (d, N1, N3, $J_{\text{N-C}} = 6.5$ Hz).

Intermediate 8: ^1H NMR (acetone- d_3 , δ 2.06 ppm) 8.25 (s, 2 H, OH), 7.77–7.34 (m, 10 H, phenyl). ^{13}C NMR (acetone- d_3 , δ 206.0 ppm) 127.3 (t, C2, $J_{\text{C-N}} = 1.5$ Hz), 162.9 (s, C4, C5). ^{15}N NMR (urea- $^{15}\text{N}_2$ δ 73.4 ppm) 364.2 (N1, N3).

Intermediate 9: ^1H NMR (acetone- d_3 , δ 2.06 ppm) 4.59 (d, 1 H, N1–H, $J_{\text{H-N1}} = 74.2$ Hz), 7.77–7.34 (m, 10 H, phenyl). ^{13}C NMR (acetone- d_3 , δ 206.0 ppm) 163.7 (d, C2, $J_{\text{C-H}} = 2.3$ Hz), 100.6 (d, C5, $J_{\text{C5-C4}} = 39.0$ Hz), 189.1 (d, C4, $J_{\text{C4-C5}} = 39.0$ Hz). ^{15}N NMR (urea- $^{15}\text{N}_2$ δ 73.4 ppm) 288.3 (d, N3, $J_{\text{N-C}} = 2.3$ Hz), 44.9 (t, N1, $J_{\text{N1-H}} = 74.0$ Hz).

1,2-Diphenylethanediimine 10: ^1H NMR (acetone- d_3 , δ 2.06 ppm) 10.31 (d, 1 H, N–H, $J_{\text{H-N}} = 54.3$ Hz), 7.77–7.34 (m, phenyl H). ^{13}C

NMR (acetone- d_3 , δ 206.0 ppm) 174.5 (C4, C5). ^{15}N NMR (urea- $^{15}\text{N}_2$ δ 73.4 ppm) 302.1 (d, N1, N3, $J_{\text{N-H}} = 54.0$ Hz). FAB/MS (m/z [M + H] $^+$): 209.1.

4,5-Diphenyl-4-hydroxyimidazol-2-one: ^{13}C NMR (acetone- d_3 , δ 206.0 ppm) **11a** 166.6 (dd, C2, $J_{\text{C2-N1}} = 15.2$ Hz, $J_{\text{C2-N3}} = 8.9$ Hz), 182.9 (d, C4, $J_{\text{C4-C5}} = 38.1$ Hz), 98.7 (dt, C5, $J_{\text{C5-C4}} = 39.2$ Hz, $J_{\text{C4-N}} = 10.3$ Hz); **11b** 165.8 (dd, C2, $J_{\text{C2-N1}} = 16.7$ Hz, $J_{\text{C2-N3}} = 10.7$ Hz), 181.0 (d, C4, $J_{\text{C4-C5}} = 31.6$ Hz), 90.8 (dt, C5, $J_{\text{C5-C4}} = 31.6$ Hz, $J_{\text{C4-N}} = 11.1$ Hz).

4,5-Diphenyl-4-methoxyimidazol-2-one 12: ^{13}C NMR (acetone- d_3 , δ 206.0 ppm) 165.8 (dd, C2, $J_{\text{C2-N1}} = 17.4$ Hz, $J_{\text{C2-N3}} = 9.8$ Hz), 186.8 (d, C4, $J_{\text{C4-C5}} = 37.7$ Hz), 95.7 (dt, C5, $J_{\text{C5-C4}} = 37.8$ Hz, $J_{\text{C4-N}} = 11.8$ Hz). ^{15}N NMR (urea- $^{15}\text{N}_2$ δ 73.4 ppm): 303.2 (N3), 120.3 (N1, $J_{\text{N1-C2}} = 16.6$ Hz).

2,5-Endoperoxide of N-Methyl-2- ^{13}C -1,3- ^{15}N -4,5-diphenylimidazole 17: (acetone- d_3 , δ 2.07 ppm) 7.61–7.22 (m, 10H, phenyl-H), 6.97, 6.58 (dd, 1H, C2–H $J_{\text{C2-H}} = 194.6$ Hz, $J_{\text{N-H}} = 3.9$ Hz), 3.84 (d, 3H, N–CH $_3$, $^3J_{\text{N-H}} = 11.7$ Hz). ^{13}C NMR (acetone- d_3 , δ 206.0 ppm): 174.6 (d, 1C, C4, $J_{\text{C-N}} = 6.5$ Hz), 105.2 (dd, 1C, C2, $^1J_{\text{C2-H}} = 194.2$ Hz, $J_{\text{C2-N}} = 4.4$ Hz), 101.3 (s, 1C, C5), 130.8, 129.2, 128.7, 128.6, 128.3, 128.2, 127.6, 127.4, 126.8, 126.7, 125.5 (12C, phenyl C), 67.7 (s, 1C, N–CH $_3$). ^{15}N NMR (urea- $^{15}\text{N}_2$ δ 73.4 ppm): 310.6 (N1), 104.6 (N3).

CO $_2$ Distribution and $^{18}\text{O}_2$ Tracer Study. Photosensitized oxidation was carried out in the same manner as above. After the solution in a 5-mm NMR tube was purged with argon, O $_2$ gas was introduced into the solution by a gastight syringe every 15 min. The NMR tube was capped with a septum rubber cap. After completion of photolysis, the NMR tube was slowly warmed to the desired temperature. A gas sample above the solution was taken with a 25- μL gastight syringe and analyzed by GC/MS. The data shown in Table 2 are the mean values of 4–5 determinations that are within $\pm 5\%$ from the mean value. See Supporting Information for the detailed calculation of the theoretical CO $_2$ distribution.

In the above calculations we assume that $^{34}\text{O}_2$ consists of two ^{17}O . $^{34}\text{O}_2$ could also consist of one ^{16}O and one ^{18}O . In that case the 2-O result is the same as above.

2-O: 4,5-diphenylimidazole $^{44}[\text{CO}_2]:^{45}[\text{CO}_2]:^{46}[\text{CO}_2]:^{48}[\text{CO}_2] =$
100:1.19:1.87:2.08

4-Methylimidazole $^{44}[\text{CO}_2]:^{45}[\text{CO}_2]:^{46}[\text{CO}_2]:^{48}[\text{CO}_2] =$
100:1.10:0.50:5.44

Imidazole $^{44}[\text{CO}_2]:^{45}[\text{CO}_2]:^{46}[\text{CO}_2]:^{48}[\text{CO}_2] =$
100:1.10:0.46:5.99

1-O is the same as above except for the $^{46}[\text{CO}_2]$ abundance.

1-O: 4,5-diphenylimidazole $^{44}[\text{CO}_2]:^{45}[\text{CO}_2]:^{46}[\text{CO}_2]:^{48}[\text{CO}_2] =$
100:1.19:8.38:0.17

4-Methylimidazole $^{44}[\text{CO}_2]:^{45}[\text{CO}_2]:^{46}[\text{CO}_2]:^{48}[\text{CO}_2] =$
100:1.10:11.38:0.32

Imidazole $^{44}[\text{CO}_2]:^{45}[\text{CO}_2]:^{46}[\text{CO}_2]:^{48}[\text{CO}_2] =$
100:1.10:12.44:0.39

Acknowledgment. We thank the NSF for support from Grant No. CHE-9730386. The Avance 500 NMR was supported by NSF CHE-9974928.

Supporting Information Available: Detailed CO $_2$ distribution calculations, ^1H – ^{15}C HMQC of **5** and **6**, ^1H , ^{13}C NMR of 1,2- ^{13}C -benzoin, ^1H , ^{13}C , ^{15}N NMR of 2,4,5- ^{13}C -1,3- ^{15}N -4,5-diphenylimidazole, ^1H , ^{13}C , ^{15}N NMR of *N*-methyl-2- ^{13}C -1,3- ^{15}N -4,5-diphenylimidazole, ^{13}C , ^{15}N NMR of reaction mixture of 2,4,5- ^{13}C -1,3- ^{15}N -4,5-diphenylimidazole at 193 K, ^{15}N NMR of 2,5-endoperoxide **5**, ^1H – ^{15}N HMQC of **5** and **9**, ^1H – ^{13}C HMBC of 2,5-endoperoxide **5** and diol intermediate **8**, ^{13}C NMR and ^1H – ^{15}N HMQC of 1,2-diphenylethanimine **10**, ^{13}C , ^{15}N NMR of 4,5-diphenyl-4-methoxyimidazol-2-one **12**, ^{13}C NMR of 4,5-diphenyl-4-hydroxyimidazol-2-one **11** (PDF). This material is available free of charge via the Internet at <http://pubs.acs.org>.

JA012253D